JOURNAL OF COMPUTATIONAL PHYSICS **129,** 181–189 (1996)
ARTICLE NO. 0242

Numerical Solutions of the Maxwell–Bloch Laser Equations

Ben-Yu Guo,* I. Martín,† Victor M. Pérez-García,‡ and Luis Vázquez§

**Department of Mathematics, City University of Hongkong, Kowloon, Hongkong; †Departamento de Informática y Automática, Universidad Complutense, E-28040, Madrid, Spain; ‡Departamento de Matemáticas, Escuela Técnica Superior de Ingenieros Industriales, Universidad de Castilla-La Mancha, Campus Universitario s/n, E-13071, Ciudad Real, Spain; Departamento de Física Teórica I, Universidad Complutense, E-28040, Madrid, Spain*

Received September 18, 1995; revised April 19, 1996

A finite difference scheme is proposed for solving the initial-boundary value problem of the Maxwell–Bloch equations. Its numerical solutions preserve some properties of the true solution. The numerical experiments are presented. Finally the stability and convergence are proved strictly.

1. INTRODUCTION

As we know, the Maxwell–Bloch equations play an important role in optics, where they describe the evolution of the slowly varying envelope of the electromagnetic field in a closed cavity filled with a resonant two-level medium [1–3]. Similar equations arise when considering active optical fibers in a very general context [4].

Let Q be the square $\{(x, y) \mid 0 < x, y < 1\}$, with the boundary ∂Q. The complex functions F and P will describe the complex electric field and matter polarization, respectively. The real-valued function D is related to the population inversion. Let i be the imaginary unit and z^* the conjugate value of z; Δ is the Laplacian and s is a rescaled time. Then the Maxwell–Bloch equations for the trasverse dynamics of a single longitudinal mode laser in the mean field approximation [2, 5] are

$$\frac{\partial F}{\partial s} - \frac{i}{4\mathscr{F}}\Delta F + \sigma(F - P) = 0, \quad (x, y) \in Q, s > 0 \tag{1}$$

$$\frac{\partial P}{\partial s} + (1 + i\delta)P - FD = 0, \quad (x, y) \in Q, s > 0 \tag{2}$$

$$\frac{\partial D}{\partial s} + \gamma\left[D - r + \frac{1}{2}(F^*P + FP^*)\right] = 0, \quad (x\, y) \in Q, s > 0. \tag{3}$$

The meaning of the parameters is the usual [5]. The nonnegative function $r(x, y, s)$ is a rescaled pumping. The constant δ is the scaled detuning. $\sigma(x, y)$ is a measure of the losses which might be constant in many practical problems. γ is a positive constant and $\gamma < 1$. $\mathscr{F}$ is a positive constant which measures the number of modes that can oscillate in the resonator. The initial data $F_0(x, y)$, $P_0(x, y)$, $D_0(x, y)$ are given. Without any loss of generality, we assume that

$$F(x, y, s) \equiv P(x, y, s) \equiv D(x, y, s) = 0, \quad (x, y) \in \partial Q, s > 0, \tag{4}$$

for a closed resonator with reflecting boundaries.

Some numerical studies for this problem have been performed using both spectral method [6, 7] and finite difference method [9]. All of these studies clarified different points of the physical dynamics. The finite difference has some advantages related to its simple implementation, its flexibility to implement different boundary conditions, the consideration of imperfection effects, etc. One of the mayor drawbacks of the numerical studies made up to now is that, none of these schemes have been constructed over a rigorous mathematical analysis of the numerical scheme properties and sometimes dubious results have arisen.

This paper deals with a finite difference scheme. Since we approximate the nonlinear terms suitably, its solution possesses some properties which are reasonable analogies of those in the continuous model. Thus it provides good numerical results. We also analyze the stability of this scheme. Usually nonlinear problems are not stable in the sense of Courant and Lax (see [10]). But they might be stable in the generalized sense given by Ben-Yu Guo (see [11–13]). As we approximate the nonlinear terms suitably in this paper the scheme possesses the best stability; i.e., the index of generalized stability is minus infinity. Accordingly, the global convergence follows. The main idea and techniques used in the theoretical analysis of this paper are also applicable to other nonlinear problems occurring in the wide area of nonlinear optics.

2. THE PROPERTIES OF THE MAXWELL–BLOCH EQUATIONS

We first analyze some properties of the solutions of the Maxwell–Bloch equations. Let $z = z_r + iz_i$, z_r and z_i being

0021-9991/96 $18.00

the real and imaginary parts of z, respectively. We can rewrite (1) as

$$\frac{\partial F_r}{\partial s} + \frac{1}{4\mathscr{F}}\Delta F_i + \sigma(F_r - P_r) = 0, \tag{5}$$

$$\frac{\partial F_i}{\partial s} - \frac{1}{4\mathscr{F}}\Delta F_r + \sigma(F_i - P_i) = 0. \tag{6}$$

Similarly, (2) stands for

$$\frac{\partial P_r}{\partial s} + P_r - \delta P_i - F_r D = 0, \tag{7}$$

$$\frac{\partial P_i}{\partial s} + P_i + \delta P_r - F_i D = 0. \tag{8}$$

Also, (3) leads to

$$\frac{\partial D}{\partial s} + \gamma[D - r + F_r P_r + F_i P_i] = 0. \tag{9}$$

Let (z_1, z_2) and $\|z\|$ be the inner product and the norm in $L^2(Q)$,

$$(z_1, z_2) = \int\int_Q z_1 z_2^* \, dxdy, \quad \|z\| = \sqrt{(z, z)}.$$

We take the inner product of (5) with F_r to obtain that

$$\frac{1}{2}\frac{\partial}{\partial s}\|F_r(s)\|^2 + \frac{1}{4\mathscr{F}}(\Delta F_i(s), F_r(s)) + \|\sqrt{\sigma}\, F_r(s)\|^2 - (\sigma, F_r(s)P_r(s)) = 0. \tag{10}$$

Similarly, (6) leads to

$$\frac{1}{2}\frac{\partial}{\partial s}\|F_i(s)\|^2 - \frac{1}{4\mathscr{F}}(\Delta F_i(s), F_r(s)) + \|\sqrt{\sigma}F_i(s)\|^2 - (\sigma, F_i(s)P_i(s)) = 0. \tag{11}$$

By boundary condition (4) and Green's formula,

$$(\Delta F_i(s), F_r(s)) = (\Delta F_r(s), F_i(s)). \tag{12}$$

Putting (10) and (11) together, we obtain

$$\frac{1}{2}\frac{\partial}{\partial s}\|F(s)\|^2 + \|\sqrt{\sigma}F(s)\|^2 - (\sigma, F_r(s)P_r(s) + F_i(s)P_i(s)) = 0. \tag{13}$$

In the same way, we deduce from (7) and (8) that

$$\frac{1}{2}\frac{\partial}{\partial s}\|P(s)\|^2 + \|P(s)\|^2 - (D(s), F_r(s)P_r(s) + F_i(s)P_i(s)) = 0. \tag{14}$$

Similarly, we get from (9) that

$$\frac{1}{2}\frac{\partial}{\partial s}\|D(s)\|^2 + \gamma\|D(s)\|^2 - \gamma(r(s), D(s)) + \gamma(D(s), F_r(s)P_r(s) + F_i(s)P_i(s)) = 0. \tag{15}$$

We multiply (14) by γ and put the resulting equation together with (13) and (15). Then

$$\frac{\partial E(s)}{\partial s} + 2\|\sqrt{\sigma}F(s)\|^2 + 2\gamma\|P(s)\|^2 + 2\gamma\|D(s)\|^2 = 2G(s) + 2\gamma\,(r(s), D(s)), \tag{16}$$

where

$$E(s) = \|F(s)\|^2 + \gamma\|P(s)\|^2 + \|D(s)\|^2,$$
$$G(s) = (\sigma, F_r(s)P_r(s) + F_i(s)P_i(s)).$$

Thus the solutions of (1)–(4) satisfy the equality

$$E(s) + 2\int_0^s (\|\sqrt{\sigma}F(s')\|^2 + \gamma\|P(s')\|^2 + \gamma\|D(s')\|^2)\, ds' = E(0) + 2\int_0^s [G(s') + \gamma(r(s'), D(s'))]\, ds'. \tag{17}$$

Remark 1. Obviously for any $0 < \alpha < 1$,

$$|G(s)| \le \alpha\|\sqrt{|\sigma|}F(s)\|^2 + \frac{1}{4\alpha}\|\sqrt{|\sigma|}P(s)\|^2. \tag{18}$$

If $\sigma(x, y) \le \sigma_1 < 4\gamma$, for all $(x, y) \in Q$, then we take $\alpha = \sigma_1/4\gamma + \varepsilon$, ε being suitably small positive constant. Thus

$$0 < \beta_1 = \min\left(1 - \frac{\sigma_1}{4\gamma} - \varepsilon, 1 - \frac{\sigma_1}{\sigma_1 + 4\varepsilon\gamma}\right) < 1. \tag{19}$$

If in addition, $\sigma(x, y) \ge \sigma_0 \ge 0$ and $r(x, y, s) \equiv 0$, then (16) reads

$$\frac{\partial E(s)}{\partial s} + 2\beta E(s) \le 0, \tag{20}$$

with

$$\beta = \min(\sigma_0\beta_1, \beta_1, \gamma).$$

Clearly in this case $E(s) \le E(0)e^{-\beta s}$, and so $E(s) \le E(0)$. In particular if $\sigma_0 > 0$, then $E(s) \to 0$ as $s \to \infty$. Physically $r(x, y, s) \equiv 0$ means the absence of pumping. If also $0 < \sigma_0 \le \sigma_1 < 4\gamma$, then the system decays as s tends to the infinity.

3. THE FINITE DIFFERENCE SCHEME

We now consider the finite difference scheme for solving (1)–(4). Let $h = 1/N$ be the mesh size in the space, N being any positive integer. The discrete domain Q_h is defined by

$$Q_h = \{(x, y) = (mh, nh) \mid 1 \le m, n \le N - 1\}$$

with the discrete boundary ∂Q_h. We introduce the discrete inner product and norm as

$$(z_1, z_2)_h = \sum_{(x,y)\in Q_h} z_1(x, y)\, z_2^*(x, y), \quad \|z\|_h = (z, z)_h^{1/2}.$$

We shall use the following notations:

$$z_x(x, y) = \frac{z(x + h, y) - z(x, y)}{h},$$

$$z_y(x, y) = \frac{z(x, y + h) - z(x, y)}{h},$$

$$z_{\bar{x}}(x, y) = z_x(x - h, y),$$

$$z_{\bar{y}}(x, y) = z_y(x, y - h),$$

$$\Delta_h z(x, y) = z_{x\bar{x}}(x, y) + z_{y\bar{y}}(x, y).$$

It is shown in [12] that for any real-valued functions u and v with homogeneuous boundary conditions, we have

$$(\Delta_h u, v)_h = (\Delta_h v, u)_h. \tag{21}$$

Furthermore, let τ be the mesh size in time s and

$$\dot{R}_\tau = \{s = k\tau, k = 1, 2, 3, ...\}, \quad R_\tau = \dot{R}_\tau \cup \{0\}.$$

We also introduce the following notations:

$$\hat{z}(x, y, s) = \frac{1}{2}(z(x, y, s + \tau) + z(x, y, s - \tau)),$$

$$\bar{z}\left(x, y, s + \frac{\tau}{2}\right) = \frac{1}{2}(z(x, y, s + \tau) + z(x, y, s)),$$

$$z_s(x, y, s) = \frac{1}{\tau}(z(x, y, s + \tau) - z(x, y, s)),$$

$$z_{\hat{s}}(x, y, s) = z_s(x, y, s - \tau),$$

$$z_{\hat{s}}(x, y, s) = \frac{1}{2}(z_s(x, y, s) + z_s(x, y, s)).$$

It is shown in [12] that

$$(z_s(s), z(s + \tau) + z(s))_h = \frac{1}{\tau}(\|z(s + \tau)\|_h^2 - \|z(s)\|_h^2) = (\|z(s)\|_h^2)_s, \tag{22}$$

$$2(z_{\hat{s}}(s), \hat{z}(s))_h = \frac{1}{2\tau}(\|z(s + \tau)\|_h^2 - \|z(s - \tau)\|_h^2) = (\|z(s)\|_h^2)_{\hat{s}}. \tag{23}$$

We begin to construct the scheme. It is commonly admitted that a reasonable discretization of a partial differential equation should preserve some properties of its genuine solution; e.g., see [11]–[14]. We shall propose a finite difference scheme, the solutions of which have the properties simulating (17). Let f, p, and d be the approximations to F, P, and D, respectively. Then the scheme is

$$f_{\hat{s}}(x, y, s) - \frac{i}{4\mathscr{F}}\Delta_h \hat{f}(x, y, s) + \sigma(x, y)\,(\hat{f}(x, y, s) - \hat{p}(x, y, s)) = 0, \quad (x, y) \in Q_h, s \in \dot{R}_\tau, \tag{24}$$

$$p_{\hat{s}}(x, y, s) + (1 + i\delta)\,\hat{p}(x, y, s) - f(x, y, s)\,\hat{d}(x, y, s) = 0, \quad (x, y) \in Q_h, s \in \dot{R}_\tau, \tag{25}$$

$$d_{\hat{s}}(x, y, s) + \gamma\hat{d}(x, y, s) - \gamma r(x, y, s) + \gamma f_r(x, y, s)\,\hat{p}_r(x, y, s) + \gamma f_i(x, y, s)\,\hat{p}_i(x, y, s) = 0, \quad (x, y) \in Q_h, s \in \dot{R}_\tau \tag{26}$$

The values of $f(x, y, \tau)$, $p(x, y, \tau)$, and $d(x, y, \tau)$ are evaluated by the corresponding Crank–Nicholson-type scheme, i.e.,

$$f_s(x, y, 0) - \frac{i}{4\mathscr{F}}\Delta_h \bar{f}\left(x, y, \frac{\tau}{2}\right) + \sigma(x, y)\left(\bar{f}\left(x, y, \frac{\tau}{2}\right) - \bar{p}\left(x, y, \frac{\tau}{2}\right)\right) = 0, \tag{27}$$

$$p_s(x, y, 0) + (1 + i\delta)\,\bar{p}\left(x, y, \frac{\tau}{2}\right) - f(x, y, 0)\,\bar{d}\left(x, y, \frac{\tau}{2}\right) = 0, \tag{28}$$

$$d_s(x, y, 0) + \gamma\bar{d}\left(x, y, \frac{\tau}{2}\right) - \gamma\bar{r}\left(x, y, \frac{\tau}{2}\right) + \gamma f_r(x, y, 0)\,\bar{p}_r\left(x, y, \frac{\tau}{2}\right) + \gamma f_i(x, y, 0)\,\bar{p}_i\left(x, y, \frac{\tau}{2}\right) = 0. \tag{29}$$

The initial values $f_0 = F_0$, $p_0 = P_0$, $d_0 = D_0$. Besides f, p, and d vanish on ∂Q_h.

Remark 2. The formula (26) is equivalent to

$$d_{\hat{s}}(x, y, s) + \gamma \hat{d}(x, y, s) - \gamma r(x, y, s) + \frac{\gamma}{2} f^*(x, y, s)\, \hat{p}(x, y, s) + \frac{\gamma}{2} f(x, y, s)\, \hat{p}^*(x, y, s) = 0.$$

It is easy to solve (24)–(29). If the values at time $s - \tau$ are known, then we evaluate $p(x, y, s)$ and $d(x, y, s)$ by (25) and (26) explicitly. Then we calculate $f(x, y, s)$ by solving a linear system (24). The fact that the scheme is linearly implicit allows the use of fast linear equation solvers as will be discussed later and saves a lot of work.

Let us check the properties of the proposed scheme. We can rewrite (24) as

$$f_{r,\hat{s}}(x, y, s) + \frac{1}{4\mathscr{T}} \Delta_h \hat{f}_i(x, y, s) + \sigma(x, y)\, (\hat{f}_r(x, y, s) - \hat{p}_r(x, y, s)) = 0, \tag{30}$$

$$f_{i,\hat{s}}(x, y, s) - \frac{1}{4\mathscr{T}} \Delta_h \hat{f}_r(x, y, s) + \sigma(x, y)\, (\hat{f}_i(x, y, s) - \hat{p}_i(x, y, s)) = 0, \tag{31}$$

We take the discrete inner product of (30) with $2\hat{f}_r(x, y, s)$ and the discrete inner product of (31) with $2\hat{f}_i(x, y, s)$. By putting the two resulting equalities together, we obtain from (21) and (23) that

$$(\|f(s)\|_h^2)_{\hat{s}} + 2\|\sqrt{\sigma}\hat{f}(s)\|_h^2 - 2(\sigma, \hat{f}_r(s)\hat{p}_r(s) + \hat{f}_i(s)\hat{p}_i(s))_h = 0. \tag{32}$$

In the same way, we get from (25) and (26) that

$$(\|p(s)\|_h^2)_{\hat{s}} + 2\|\hat{p}(s)\|_h^2 - 2(\hat{d}(s), f_r(s)\hat{p}_r(s) + f_i(s)\hat{p}_i(s))_h = 0, \tag{33}$$

$$(\|d(s)\|_h^2)_{\hat{s}} + 2\gamma\|\hat{d}(s)\|_h^2 - 2\gamma(r(s), \hat{d}(s))_h + 2\gamma(\hat{d}(s), f_r(s)\hat{p}_r(s) + f_i(s)\hat{p}_i(s))_h = 0. \tag{34}$$

We multiply (33) by the constant γ and put the result together with (32) and (34). Then we find that

$$(E_h(s))_{\hat{s}} + 2\|\sqrt{\sigma}\hat{f}(s)\|_h^2 + 2\gamma\|\hat{p}(s)\|_h^2 + 2\gamma\|\hat{d}(s)\|_h^2 = 2G_h(s) + 2\gamma(r(s), \hat{d}(s))_h, \tag{35}$$

where

$$E_h(s) = \|\hat{f}(s)\|_h^2 + \gamma\|\hat{p}(s)\|_h^2 + \|\hat{d}(s)\|_h^2,$$
$$G_h(s) = (\sigma, \hat{f}_r(s)\hat{p}_r(s) + \hat{f}_i(s)\hat{p}_i(s))_h.$$

By summing (35) over all $s' \le s$ we obtain

$$E_h(s + \tau) + E_h(s) + 4\tau \sum_{s'=\tau}^{s} (\|\sqrt{\sigma}\hat{f}(s')\|_h^2 + \gamma\|\hat{p}(s')\|_h^2 + \gamma\|\hat{d}(s')\|_h^2) = E_h(\tau) + E_h(0) + 4\tau \sum_{s'=\tau}^{s} (G_h(s') + \gamma(r(s'), d(s'))_h). \tag{36}$$

Clearly the above equality is a reasonable analogy of (17). Thus this scheme could provide reasonable numerical simulations.

Remark 3. We can evaluate $E_h(\tau)$ by (27)–(28) similarly. In particular, if $r(x, y, s) \equiv 0$ and $0 < \sigma_0 \le \sigma_1 \le 4\gamma$, then $E_h(s) \to 0$ as $s \to \infty$. Therefore, in this case, the discrete model also decays as the continuous model.

Remark 4. We can calculate $p(x, y, s)$ more precisely. It means that, instead of (28) and (29), we use the approximation

$$p_s(x, y, 0) + (1 + i\delta)\, \bar{p}\left(x, y, \frac{\tau}{2}\right) - \bar{f}\left(x, y, \frac{\tau}{2}\right) \bar{d}\left(x, y \frac{\tau}{2}\right) = 0, \tag{37}$$

$$d_s(x, y, 0) + \gamma \bar{d}\left(x, y, \frac{\tau}{2}\right) - \gamma \bar{r}\left(x, y, \frac{\tau}{2}\right) + \gamma \bar{f}_r\left(x, y, \frac{\tau}{2}\right) \bar{p}_r\left(x, y, \frac{\tau}{2}\right) + \gamma \bar{f}_i\left(x, y, \frac{\tau}{2}\right) \bar{p}_i\left(x, y, \frac{\tau}{2}\right) = 0. \tag{38}$$

It can be verified that there exist the unique solutions $f(x, y, \tau)$, $p(x, y, \tau)$, and $d(x, y, \tau)$ for all sufficiently small h and τ. But we will find out in Section 7 that the scheme (24)–(29) possesses the same convergence rate as the scheme defined by (24)–(27) and (37)–(38).

4. COMPUTATIONAL IMPLEMENTATION

The linear system arising from the discretization has been solved using a multigrid technique. Multigrid iterative

methods reach the solution after a fixed number of iterations; i.e., their convergence rate is independent of the number of equations N. In fact, they reach the solution of the linear system with an optimal complexity: $O(N)$ operations for an N-equation problem. Additionally they have very good parallel properties. To implement the multigrid method it is necessary to find several parameters of the algorithm. In our case, as we are working with complex functions, it is more difficult to find the adequate parameters to get the optimal complexity.

The main idea in all multigrid methods is that relaxation methods are very effective at reducing the high frequency components of the error, but it is not so with the low frequency ones (''smooth'' methods). However, these low frequency modes have higher frequency on a coarser grid and can be effectively reduced using a ''smooth'' method over that grid. This can be done in a recursive way until a certain level, where the system will be easier to solve than the original one. The Jacobi method was used to solve the system on the coarser grid ($N_i \times N_i$).

The MVJ algorithm (defined recursively by Algorithm 1) is a V-cycle basic iteration [15]. We start with an initial solution v^h and the solution is reached after a fixed number of MVJ cycles. Smoothing, restriction (I_h^{2h}), and prolongation (I_{2h}^h) operators were chosen to keep good convergence rates and to get good parallel properties. This algorithm has been successfully used, as an internal solver with a self-adaptative method, to solve the nonlinear Schrodinger equation [16].

ALGORITHM 1. $v^h \leftarrow MVJ^h(v^h, f^h)$.

1. If Ω^h is the grid with a $N_i \times N_i$ grid, solve the linear system using Jacobi and return.
2. Relax (smooth method) n_1 times $A^h u^h = f^h$ with initial guess v^h
3. $f^{2h} \leftarrow I_h^{2h}(f^h - A^h v^h), v^{2h} \leftarrow 0, v^{2h} \leftarrow MVJ^{2h}(v^{2h}, f^{2h})$
4. Correct $v^h \leftarrow v^h + I_{2h}^h v^{2h}$
5. Relax (smooth method) n_2 times on $A^h u^h = f^h$ with initial guess v^h.

If we define the problem on grids of various sizes, we can obtain the solution at each level, from the coarser grid to the finer ones, with n_0 MVJ cycles using as a first approximation the interpolated one from coarser grids. This is the full multigrid algorithm (Algorithm 2). With this approach, the solution at each level converges up to the *level of truncation* [17].

ALGORITHM 2. $v^h \leftarrow FMVJ^h(v^h, f^h)$.

1. If Ω^h is the grid with a $N_i \times N_i$ grid, solve the linear system using Jacobi $v^h \leftarrow (A^h)^{-1} f^h$ and return.
2. $v^{2h} \leftarrow FMVJ(v^{2h}, f^{2h})$
3. Correct $v^h \leftarrow v^h + I_h^{2h} v^{2h}$
4. $v^h \leftarrow MVJ(v^h, f^h)$, n_0 times.

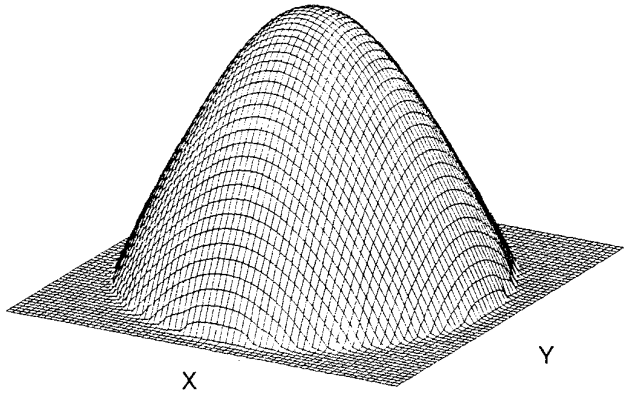

FIG. 1. Stationary TEM_{00} structure obtained for parameter values $r = 15$, $\delta = 3.65$, $\gamma = 0.1$, $\mathscr{T} = 4$, and $\sigma = 0.1$; integration parameters $\tau = 0.05$, $N = 64 \times 64$.

5. NUMERICAL RESULTS

The lack of exact results of the Maxwell–Bloch equations makes it difficult to check the numerical scheme behavior when it is applied to interesting physical problems. There are, however, some properties which are expected to be kept by the solutions and some regimes where some theoretical predictions can be done [18]. These predictions allow us to specify what the stationary solution will be for low Fresnel numbers and single longitudinal mode lasers.

Let us perform some numerical simulations. In the figures to be presented we show the laser intensity profile at a given time: $I(x, y) = |F(x, y, s)|^2$. Starting with $r = 15$, $\delta = 3.65$, $\gamma = 0.1$, $\mathscr{T} = 4$, and $\sigma = 0.1$ we obtain a stationary TEM_{00} structure at $s = 800$ computed with $\tau = 0.05$ and a spatial grid of 64×64 points (Fig. 1) which also agrees with the prediction of the theoretical model studied in [18] and the results obtained with the finite difference scheme studied in [9].

On the other hand when the physical parameters are set to $r = 60$, $\delta = 7.61$, $\mathscr{T} = 4$, $\sigma = 0.1$, $\gamma = 0.1$, which physically correspond to a multimode competition state (leading finally to an asymmetric structure), we again succeed in obtaining the right stationary solution, which has radial symmetry and zero at a given radial distance. But this time the time step needs to be reduced to $\tau = 0.0005$ (Fig. 2). Use of a larger step, $\tau = 0.005$, leads to a splitting of the numerical solution which is a typical problem of three level finite difference schemes.

Other successful simulations have been performed with parameter values $r = 12.4$, $\gamma = 0.1$, $\sigma = 0.1$, $\delta = 3.65$, $\mathscr{T} = 4$, which lead to a multimode oscillation regime of the laser (Fig. 3a for $s = 3$, b for $s = 7$, and c for $s = 14$) and $r = 3$, $\gamma = 0.1$, $\sigma = 0.1$, $\delta = 3.67$, $\mathscr{T} = 4$, which gives an asymmetric structure in the asymptotic time region (Fig. 4). These computations have been performed using a time step of $\tau = 0.005$ and spatial grids of 64×64 points.

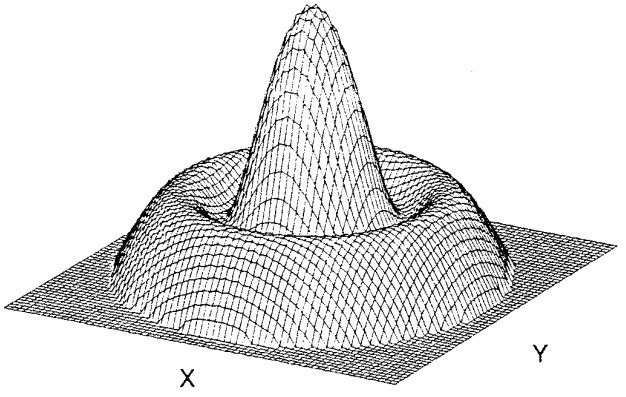

FIG. 2. Asymptotic profile for parameter values $r = 60$, $\delta = 7.61$, $\mathscr{T} = 4$, $\sigma = 0.1$, $\gamma = 0.1$; integration parameters $\tau = 0.005$, $N = 64 \times 64$.

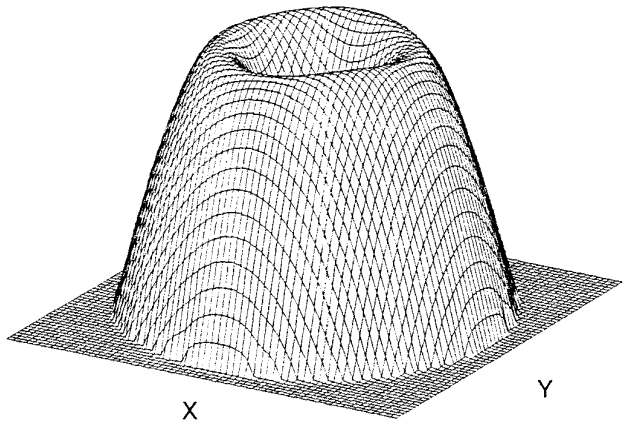

FIG. 4. Stationary profile found for $r = 3$, $\gamma = 0.1$, $\sigma = 0.1$, $\delta = 3.67$, $\mathscr{T} = 4$.

Additionally we have checked the effect of a dark spot on the laser profile, which is modelled by a region of high losses placed asymmetrically. This phenomenon has been studied experimentally by Tamm [19] and the selection of an asymmetric stationary structure with two peaks was found. In our case we have performed the numerical simulation with parameter values $\delta = -0.1$, $\sigma = 4.0$, $\gamma = 1.0$, $r = 8$, $\mathscr{T} = 8$, $\tau = 0.0005$ and the numerical result shown in Fig. 5 closely resembles the experimental result obtained by Tamm and other previous numerical results [9].

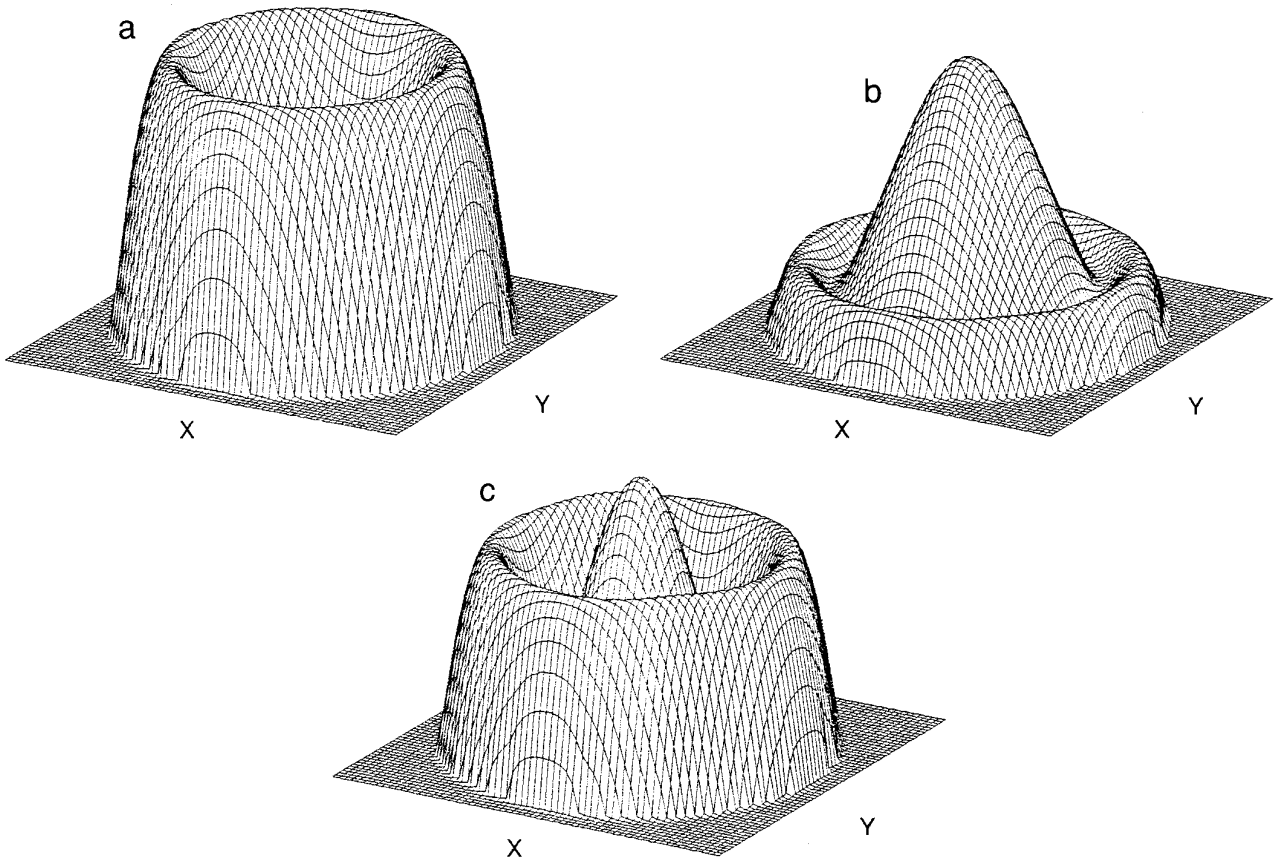

FIG. 3. Spatial profile of the laser intensity for parameter values $r = 12.4$, $\gamma = 0.1$, $\sigma = 0.1$, $\delta = 3.65$, $\mathscr{T} = 4$ computed with $\tau = 0.005$. Three different times are presented (a) $s = 3.0$, (b) $s = 7.0$, (c) $s = 14.0$.

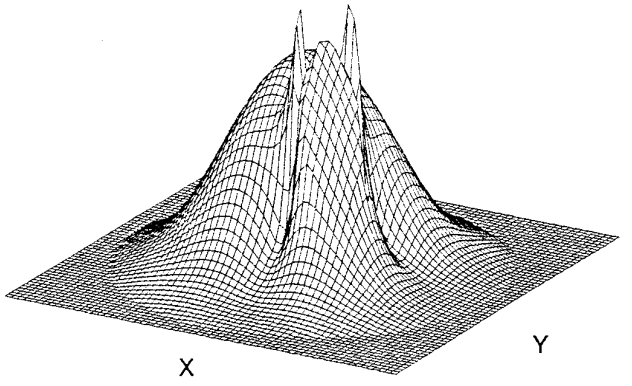

FIG. 5. Stationary profile found when the effect of an imperfection is considered. Parameter values $\delta = -0.1$, $\sigma = 4.0$, $\gamma = 1.0$, $r = 8$, $\mathscr{T} = 8$; simulation values $\tau = 0.0005$, $N = 64 \times 64$.

These simulations have been performed with 64×64 spatial grids, but in most cases the scheme works fine with spatial grids of 32×32. This means that the scheme is spatially very robust even though the order of spatial convergence is not very high, as will be shown later.

To summarize the scheme's practical behavior we must say that the linear character of the finite difference scheme makes it very fast to solve using multigrid techniques and paralellization. These are great advantages when real massive simulations are performed or computation intensive parameter regions such as turbulent ones are to be studied. In this sense this finite difference scheme outperforms the spectral schemes because of its parallelization properties and the easiness for the introduction of imperfection, gain or loss asymmetries, etc. The behavior of the scheme is right and it converges to the correct solution when the spatial and temporal steps are reasonable.

6. STABILITY ANALYSIS

As pointed out in [12], nonlinear finite difference schemes are not stable in the sense of Courant and Lax usually. But they might be stable in the sense of generalized stability. Now assume that the initial values f_0, p_0, and d_0 have the errors $\tilde{f}_0$, $\tilde{p}_0$, and $\tilde{d}_0$. The right sides of (24)–(29) have the errors $\tilde{g}_0, \tilde{g}_1, \tilde{g}_2, \tilde{q}_0, \tilde{q}_1, \tilde{q}_2$. Then the corresponding solutions f, p, and d become $f + \tilde{f}$, $p + \tilde{p}$, and $d + \tilde{d}$. By (24)–(26), we know that for $s \in \dot{R}_\tau$, the errors satisfy the equations

$$\tilde{f}_{\dot{s}}(x,y,s) - \frac{i}{4\mathscr{T}}\Delta\hat{\tilde{f}}(x,y,s) + \sigma(x,y)\,\hat{\tilde{f}}\left(x,y,\frac{\tau}{2}\right) - \sigma(x,y)\,\hat{\tilde{p}}(x,y,s) = \tilde{g}_0(x,y,s), \tag{39}$$

$$\tilde{p}_{\dot{s}}(x,y,s) + (1+i\delta)\,\hat{\tilde{p}}(x,y\,s) - (f(x,y,s) + \tilde{f}(x,y,s))\,\hat{\tilde{d}}(x,y\,s) = \tilde{g}_1(x,y,s) + \tilde{g}_3(x,y,s), \tag{40}$$

$$\tilde{d}_{\dot{s}}(x,y,s) + \gamma\hat{\tilde{d}}(x,y,s) + \gamma(f_r(x,y,s) + \tilde{f}_r(x,y,s))\,\hat{\tilde{p}}_r(x,y,s) + \gamma(f_i(x,y,s) + \tilde{f}_i(x,y,s))\,\hat{\tilde{p}}_i(x,y,s) = \tilde{g}_2(x,y,s) + \tilde{g}_4(x,y,s), \tag{41}$$

where

$$\tilde{g}_3(x,y,s) = \tilde{f}(x,y,s)\,\hat{d}(x,y,s), \tag{42}$$

$$\tilde{g}_4(x,y,s) = -\gamma\tilde{f}_r(x,y,s)\,\hat{p}_r(x,y,s) - \gamma\tilde{f}_i(x,y,s)\,\hat{p}_i(x,y,s). \tag{43}$$

Also by (27)–(29),

$$\tilde{f}_{\dot{s}}(x,y,0) - \frac{i}{4\mathscr{T}}\Delta\bar{\tilde{f}}\left(x,y,\frac{\tau}{2}\right) + \sigma(x,y)\,\bar{\tilde{f}}\left(x,y,\frac{\tau}{2}\right) - \sigma(x,y)\,\bar{\tilde{p}}\left(x,y,\frac{\tau}{2}\right) = \tilde{q}_0(x,y), \tag{44}$$

$$\tilde{p}_{\dot{s}}(x,y,0) + (1+i\delta)\,\bar{\tilde{p}}\left(x,y,\frac{\tau}{2}\right) - (f_0(x,y) + \tilde{f}_0(x,y))\,\bar{\tilde{d}}\left(x,y,\frac{\tau}{2}\right) = \tilde{g}_1(x,y) + \tilde{g}_3(x,y), \tag{45}$$

$$\tilde{d}_{\dot{s}}(x,y,0) + \gamma\bar{\tilde{d}}\left(x,y,\frac{\tau}{2}\right) + \gamma(f_{0r}(x,y) + \tilde{f}_{0r}(x,y))\,\bar{\tilde{p}}_r\left(x,y,\frac{\tau}{2}\right) + \gamma(f_{0i}(x,y) + \tilde{f}_{0i}(x,y))\,\bar{\tilde{p}}_i\left(x,y,\frac{\tau}{2}\right) = \tilde{q}_2(x,y) + \tilde{q}_4(x,y), \tag{46}$$

where

$$\tilde{q}_3(x,y) = \tilde{f}_0(x,y)\,\bar{d}\left(x,y,\frac{\tau}{2}\right),$$

$$\tilde{q}_4(x,y) = -\gamma\tilde{f}_{0r}(x,y)\,\bar{p}_r\left(x,y,\frac{\tau}{2}\right) - \gamma\tilde{f}_{0i}(x,y)\,\bar{p}_i\left(x,y,\frac{\tau}{2}\right).$$

Besides $\tilde{f}$, $\tilde{p}$, and $\tilde{d}$ vanish on ∂Q_h.

By comparing (39)–(41) to (24)–(26) and an argument similar to the derivation of (35), we conclude that

$$(\tilde{E}_h(s))_{\hat{s}} + 2\|\sqrt{\sigma}\hat{\tilde{f}}(s)\|_h^2 + 2\gamma\|\hat{\tilde{p}}(s)\|_h^2 + 2\gamma\|\hat{\tilde{d}}(s)\|_h^2 = 2\sum_{j=1}^{3} G_h^{(j)}(s), \tag{47}$$

where

$$\begin{aligned}
\tilde{E}_h(s) &= \|\tilde{f}(s)\|_h^2 + \gamma\|\tilde{p}(s)\|_h^2 + \|\tilde{d}(s)\|_h^2,\\
\tilde{G}_h^{(1)}(s) &= (\sigma, \hat{\tilde{f}}_r(s)\hat{\tilde{p}}_r(s) + \hat{\tilde{f}}_i(s)\hat{\tilde{p}}_i(s))_h,\\
\tilde{G}_h^{(2)}(s) &= (\tilde{g}_{0r}(s), \hat{\tilde{f}}_r(s))_h + (\tilde{g}_{0i}(s), \hat{\tilde{f}}_i(s))_h\\
&\quad + \gamma(\tilde{g}_{1r}(s), \hat{\tilde{p}}_r(s))_h + \gamma(\tilde{g}_{1i}(s), \hat{\tilde{p}}_i(s))_h\\
&\quad + (\tilde{g}_{2r}(s), \hat{\tilde{d}}(s))_h,\\
\tilde{G}_h^{(3)}(s) &= \gamma(\tilde{f}_r(s)\hat{\tilde{p}}_r(s) + \tilde{f}_i(s)\hat{\tilde{p}}_i(s), \hat{d}(s))_h\\
&\quad - \gamma(\tilde{f}_r(s)\hat{p}_r(s) + \tilde{f}_i(s)\hat{p}_i(s), \hat{\tilde{d}}(s))_h.
\end{aligned}$$

Let $s_1 > 0$ and $|p(x, y, s)| \le p_1$, $|d(x, y, s)| \le d_1$ for all $(x, y) \in Q_h$ and $s \le s_1 + \tau$. It can be shown that

$$|\tilde{G}_h^{(1)}(s)| \le \frac{\sigma_1^2}{2\gamma}\|\hat{\tilde{f}}(s)\|_h^2 + \frac{\gamma}{2}\|\hat{\tilde{p}}(s)\|_h^2,$$

$$|\tilde{G}_h^{(2)}(s)| \le \|\hat{\tilde{f}}(s)\|_h^2 + \frac{\gamma}{4}\|\hat{\tilde{p}}(s)\|_h^2 + \frac{\gamma}{2}\|\hat{\tilde{d}}(s)\|_h^2 + \frac{1}{2}\tilde{G}_h(s),$$

$$|\tilde{G}_h^{(3)}(s)| \le \gamma(d_1^2 + p_1^2)\,\|\tilde{f}(s)\|_h^2 + \frac{\gamma}{4}\|\hat{\tilde{p}}(s)\|_h^2 + \frac{\gamma}{2}\|\hat{\tilde{d}}(s)\|_h^2,$$

where

$$\tilde{G}_h(s) = \frac{1}{2}\|\tilde{g}_0(s)\|_h^2 + 2\gamma\|\tilde{g}_1(s)\|_h^2 + \frac{1}{\gamma}\|\tilde{g}_2(s)\|_h^2.$$

By substituting the above estimates into (47), it follows that

$$(\tilde{E}_h(s'))_{\hat{s}} \le \left(\frac{\sigma_1^2}{\gamma} + 2\sigma_1 + 2\right)\|\hat{\tilde{f}}(s')\|_h^2 + 2\gamma(d_1^2 + p_1^2)\,\|\tilde{f}(s')\|_h^2 + \frac{1}{4}\tilde{G}_{\mathrm{h}}(s'). \tag{48}$$

Let $\beta_1 = \sigma_1^2/\gamma + 2\sigma_1 + 2$ and notice that $\|\hat{\tilde{f}}(s)\|_h^2 \le \frac{1}{2}\|\tilde{f}(s+\tau)\|_h^2 + \frac{1}{2}\|\tilde{f}(s-\tau)\|_h^2$. By summing up (48) over all s' such that $\tau \le s' \le s - \tau$, we get

$$(1 - \beta_1\tau)\,(\tilde{E}_h(s) + \tilde{E}_h(s-\tau)) \le \rho_h^0(s) + \beta_2\tau\sum_{s'=\tau}^{s-\tau}\|\tilde{f}(s')\|_h^2,$$

where $\beta_2 = 2\beta_1 + 4\gamma(d_1^2 + p_1^2)$ and

$$\rho_h^0(s) = \tilde{E}_h(0) + \tilde{E}_h(\tau) + (1 + \beta_1\tau)\|\tilde{f}_0\|_h^2 + \tau\sum_{s'=\tau}^{s-\tau}\tilde{G}_h(s').$$

Let τ be suitably small such that $1 - \beta_1\tau > \frac{1}{2}$. Then

$$\tilde{E}_h(s) \le 2\rho_h^0(s) + 2\beta_2\tau\sum_{s'=\tau}^{s-\tau}\|\tilde{f}(s')\|_h^2. \tag{49}$$

Next, by (21)–(22) and an argument similar to the derivation of (48), we deduce from (44)–(46) that

$$\tilde{E}_h(\tau) \le \beta_3\tilde{E}_h(0) + \beta_4(\|\tilde{q}_0\|_h^2 + \|\tilde{q}_1\|_h^2 + \|\tilde{q}_2\|_h^2), \tag{50}$$

β_3 and β_4 being positive constants depending only on γ, σ_1, d_1, and p_1. Finally, we use the discrete Gronwall equality (see [12]) to conclude that

THEOREM 1. *Let τ be suitably small. Then for any $s_1 > 0$, all $s \le s_1$, and $\rho_h(s)$*

$$\tilde{E}_h(s) \le \beta_5\rho_h(s)e^{\beta_6 s}. \tag{51}$$

Remark 5. Theorem 1 shows the stability of scheme (24)–(29). Since β_1 and β_2 depend on p_1 and d_1, this stability is different from the stability in the sense of Courant and Lax. But there is no restriction on the data error $\rho_h(s)$. So this scheme possesses the generalized stability with the minus infinity index (see [12]). It is the best result for generalized stability.

Remark 6. Since we approximate the Maxwell–Bloch laser equations suitably, the effect of the main nonlinear error terms (such as $\tilde{f}_r(x, y, s)\,\hat{\tilde{p}}(x, y, s)$, etc.) are cancelled. Thus we get the best result.

7. THE CONVERGENCE

In this section, we deal with the convergence. Let $\tilde{g}_0, \tilde{g}_1, \tilde{g}_2, \tilde{q}_0, \tilde{q}_1, \tilde{q}_2$ denote the approximation errors of (24)–(29), respectively. Then for $s \le s_1$, $\tilde{g}_0$, $\tilde{g}_1$, $\tilde{g}_2$, $\tilde{q}_0$ are of order $O(\tau^2 + h^2)$, provided that $F, P, D \in C^2(0, s; C^4(Q))$, $\tilde{g}, \tilde{q} \in C^2(0, s; C^0(Q))$. While $\tilde{q}_1$, $\tilde{q}_2$ are of order $O(\tau + h^2)$. Let $\tilde{F} = f - F$, $\tilde{P} = p - P$, $\tilde{D} = d - D$. Then by (1)–(3) and (24)–(29) the errors satisfy the equations similar to (39)–(46). But $\tilde{f}$, $\tilde{p}$, and $\tilde{d}$ are replaced by $\tilde{F}$, $\tilde{P}$, and $\tilde{D}$, respectively. On the other hand, $\tilde{g}_0$, $\tilde{g}_1$, $\tilde{g}_2$, $\tilde{q}_0$, $\tilde{q}_1$, and $\tilde{q}_2$ are replaced by $-\tilde{g}_0$, $-\tilde{g}_1$, $-\tilde{g}_2$, $-\tilde{q}_0$, $-\tilde{q}_1$, and $-\tilde{q}_2$. Besides $\tilde{F} \equiv \tilde{P} \equiv \tilde{D} = 0$ at $s = 0$. We also get a similar error estimation, but $\tilde{E}_h(s)$ and $\rho_h(s)$ are given by

$$\tilde{E}_h(s) = \|\tilde{F}(s)\|_h^2 + \gamma\|\tilde{P}(s)\|_h^2 + \|\tilde{D}(s)\|_h^2,$$

$$\rho_h(s) = \tau \sum_{s'=\tau}^{s-\tau} (\|\tilde{g}_0(s')\|_h^2 + \|\tilde{g}_1(s')\|_h^2 + \|\tilde{g}_2(s')\|_h^2) + \tau \sum_{j=0}^{2} \|\tilde{q}_j\|_h^2. \tag{52}$$

Also d_1 and p_1 are replaced by D_1 and P_1:

$$D_1 = \max_{(x,y)\in Q, s\le s_1+\tau} |D(x, y, s)|,$$

$$P_1 = \max_{(x,y)\in Q, s\le s_1+\tau} |P(x, y, s)|.$$

THEOREM 2. *If τ is suitably small, then for all $s \le s_1$ and $\rho_h(s)$,*

$$\tilde{E}_h(s) \le \beta_7 \rho_h(s) e^{\beta_8 s},$$

β_7 and β_8 being positive constants depending only on γ, σ_1, P_1, and D_1.

Remark 7. By (52), $\rho_h(s) = O(\tau^3 + h^4)$. Thus we get the convergence rate with the order $O(\tau^{3/2} + h^2)$. Since theorem holds for any $s > 0$, Theorem 2 implies the global convergence.

Remark 8. If we use the scheme (24)–(26) and (37)–(38) then we get the same generalized stability, but the convergence rate is $O(\tau^2 + h^4)$.

Remark 9. If the boundary values are not zero, Theorem 1 and Theorem 2 are still valid.

8. CONCLUSIONS

We have derived and studied a finite difference scheme for the Maxwell–Bloch equations. From the practical viewpoint this scheme is linearly implicit, which allows multigrid techniques to be applied, thus greatly enhancing the computational performance. The fact that it is a finite difference method allows the effects of imperfections, nontrivial gain or loss profiles, etc. to be easily considered. From the mathematical side it is also interesting that we have been able to prove the stability and convergence of the scheme and that it posseses discrete variation laws that are analogous to the continuous ones. Because of its good computational performance and mathematical properties we hope that this scheme will be useful when addressing the simulation of very disordered states recently found in real lasers [20] which can be properly called turbulent.

ACKNOWLEDGMENTS

B-Y. G. acknowledges support from the Universidad Complutense through its sabatical programme. I. M. acknowledges support from Grant TAP-0832-C02-01. V.M.T.-G acknowledges partial support from the DGICT under Grant PB92-0798. L.V. is partially supported by the DGICT through Grant PB92-0226.

REFERENCES

1. H. Haken, "Light," Vol. 2, North-Holland, Amsterdam, 1985.
2. L. A. Lugiato, G. L. Oppo, J. R. Tredicce, L. M. Narducci, and M. A. Pernigo, *J. Opt. Soc. Am. B* **7,** 1019 (1990).
3. A. C. Newell and J. V. Moloney, "Nonlinear Optics," Addison-Wesley, Redwood, CA, 1992.
4. V. M. Pérez-García, thesis, Universidad Complutense, Madrid, 1995 (unpublished).
5. V. M. Pérez-García and J. M. Guerra, *Phys. Rev. A* **50,** 1646 (1994).
6. P. Coullet, L. Gil, and F. Rocca, *Opt. Commun.* **73,** 403 (1989).
7. E. J. D'Angelo, C. Green, J. R. Tredicce, N. B. Abraham, S. Balle, Z. Chen, and G. L. Oppo, *Physica D* **61,** 6 (1992).
8. R. Indik and A. C. Newell, *Math. Comput. Simul.* **37,** 370 (1994).
9. I. Martín, V. M. Pérez-García, J. M. Guerra, F. Tirado, and L. Vázquez, in *Fluctuation Phenomena: Disorder and Nonlinearity,* edited by A. R. Bishop, S. Jiménez, and L. Vázquez (World Scientific, Singapore, 1995), p. 390.
10. R. D. Ritchmyer and K. W. Morton, *Finite Difference Methods for Initial Value Problems,* 2nd ed. (Interscience, New York, 1967).
11. B. Y. Guo, Tech. Report of the SUST, 1965; *Acta Math. Sinica* **17,** 242 (1974).
12. B. Y. Guo, *Difference Methods for Partial Differential Equations* (Science, Beijing, 1988).
13. B. Y. Guo and L. Vázquez, *J. Appl. Sci.* **1,** 25 (1983).
14. P.-Y. Kuo and H.-M. Wu, *J. Math. Anal. Appl.* **81,** 334 (1981).
15. R. Golub and J. Ortega, *Scientific Computing, An Introduction with Parallel Computing* (Academic Press, New York, 1993).
16. I. Martín, F. Tirado, L. Vázquez, and J. C. Fabero, in *VI International Conference on Physics Computing,* 1995.
17. W. L. Briggs, *Multigrid Tutorial* (SIAM, Philadelphia, 1987).
18. O. Gómez-Calderón, V. M. Pérez-García, I. Martín, and J. M. Guerra, *Phys. Rev. A,* to appear.
19. C. Tamm, *Phys. Rev. A* **38,** 5960 (1988).
20. V. M. Pérez-García, I. Pastor, and J. M. Guerra, *Phys. Rev. A* **52,** 2392 (1995).